Skeletal Radiology (2024) 53:67–73
https://doi.org/10.1007/s00256-023-04376-7

SCIENTIFIC ARTICLE

MRI 3D simulation of hip motion in female patients with and without ischiofemoral impingement

Till D. Lerch[1] · Florian A. Huber[2,3] · Miriam A. Bredella[2] · Simon D. Steppacher[1] · Moritz Tannast[1] · Joao R. T. Vicentini[2] · Martin Torriani[2]

Received: 11 April 2023 / Revised: 28 May 2023 / Accepted: 28 May 2023 / Published online: 3 June 2023

Abstract

Objective To utilize hip MRI 3D models for demonstration of location and frequency of impingement during simulated range-of-motion in ischiofemoral impingement (IFI) compared to non-IFI hips.

Materials and methods Sixteen hips ($N = 7$ IFI, 9 non-IFI) from 8 females were examined with high-resolution MRI. We performed image segmentation and generated 3D bone models and simulated hip range-of-motion and impingement. We examined the frequency and location of bone contact in early external rotation and early extension (0–20°), isolated maximum external rotation, and isolated maximum extension. Frequency and location of impingement at varied combinations of external rotation and extension and areas of simulated bone impingement at early external rotation and extension were compared between IFI and non-IFI.

Results Higher frequency of bony impingement occurred more often in IFI hips at each simulated range-of-motion combination ($P < 0.05$). Impingement involved the lesser trochanter more often in IFI hips ($P < 0.001$) and occurred at early degrees of external rotation and extension. In isolated maximum external rotation, only the greater trochanter, intertrochanteric area, or both combined were involved, in 14%, 57%, and 29% in IFI hips. In isolated maximum extension, the lesser trochanter, intertrochanteric area, or both combined were involved in 71%, 14%, and 14% in IFI hips. The simulated area of bone impingement was significantly higher in IFI hips ($P = 0.02$).

Conclusion Hip MRI 3D models are feasible for simulated range-of-motion and show a higher frequency of extra-articular impingement at early stages of external rotation and extension in IFI compared to non-IFI hips.

Keywords Magnetic resonance imaging · Computer-assisted diagnosis · Joint range of motion · Hip impingement · Lesser trochanter

Abbreviations

FAI	Femoroacetabular impingement
IFI	Ischiofemoral impingement
QF	Quadratus femoris
ROM	Range of motion

Introduction

Ischiofemoral impingement (IFI) is recognized as a cause of posterior hip pain and quadratus femoris (QF) muscle abnormalities due to narrowing between the lesser trochanter (LT) and ischial tuberosity or hamstring origin [1]. It is described mainly in female patients limiting extension and long-stride walking [2, 3]. Recent investigations have demonstrated the utility of CT-based 3D modeling to better understand the dynamics of other hip impingement phenomena. For

Till D. Lerch and Florian A. Huber contributed equally to this work.

✉ Martin Torriani
mtorriani@mgh.harvard.edu

[1] Department of Diagnostic, Interventional and Pediatric Radiology, University Hospital of Bern, Inselspital, University of Bern, Freiburgstrasse 10, 3010 Bern, Switzerland

[2] Division of Musculoskeletal Imaging and Intervention, Department of Radiology, Massachusetts General Hospital and Harvard Medical School, 55 Fruit St, Boston, MA 02114, USA

[3] Institute of Diagnostic and Interventional Radiology, University Hospital Zurich, Raemistrasse 100, 8091 Zurich, Switzerland

example, in femoroacetabular impingement (FAI), bony prominences of the acetabulum and femur have been shown to contact significantly more often and at lower degrees of flexion, internal rotation with 90° of flexion, and abduction [4]. In IFI, the 3D relationships between LT and ischium depend on multiple factors, including femoral version [5], pelvic morphology [3], and degree of hip external rotation and extension [6]. As a consequence, the features of bony contact in IFI may vary as a function of hip external rotation and extension. For example, bony contact in IFI may occur early in hip range of motion (ROM), and extra-articular points of contact besides the ischial tuberosity and LT may involve the greater trochanter (GT) and intertrochanteric region [7]. Better understanding of the 3D anatomy in IFI and its potential effect on ROM may promote better clinical management and surgical planning without the use of ionizing radiation.

To our knowledge, no studies have evaluated the 3D anatomy of IFI hips by means of simulated ROM derived from MRI data. The purpose of this study was to use 3D MRI to investigate the location and frequency of impingement in IFI hips. We sought to evaluate the location and degree of external rotation and extension at which bony contact occurs in IFI compared to normal hips. We hypothesized that simulated ROM in IFI shows impingement at early stages of external rotation and extension compared to normal hips and that areas of bony contact in the femur are not limited to the LT.

Materials and methods

This retrospective study was approved by the institutional review board with a waiver for informed consent and was performed in compliance with the Health Insurance Portability and Accountability Act (HIPAA) as well as in accordance with the Declaration of Helsinki.

In a prior study, a cohort of 12 women (24 hips) underwent a prospective kinematic MRI study to investigate IFI between March 2017 and May 2018 [6]. That cohort comprised of individuals with and without IFI, based on measurements of the ischiofemoral and the QF spaces [8]. A subset of these subjects performed a previously unreported 3D high-resolution T1-weighted gradient-echo Dixon MR sequence, which was used for the current study that differs from the prior study by evaluating 3D models and simulated motion. The 3D-MRI parameters were as follows: axial acquisition, echo time (4.9 ms), repetition time (12.3 ms), voxel size (1.97×1.97×1 mm), matrix (192×192), field-of-view (38×38 cm), and acquisition time (4:47 min). A T2-weighted fat-suppressed axial pulse sequence through the pelvis was also available (echo time: 68 ms, repetition time: 3000 ms, matrix: 320×240, field-of-view: 36×27 cm, acquisition time: 1:59 min). The presence of edema in the QF muscle was evaluated on the T2-weighted images by a radiologist with 6 years of musculoskeletal experience (FAH). Symptomatic patients were identified by medical chart review of electronic health records.

Bone segmentation was performed manually on 3D high-resolution T1-weighted MR images of all study participants using ITK Snap, version 3.8.0 [9]. Bone segmentation was performed by a radiologist with 6 years of experience (FAH) and reviewed and changed where applicable by a second radiologist with 6 years of experience in IFI-related research (TDL). Subsequently, 3D models were created for all segmentation masks and exported as STL files. The 3D models were loaded in a proprietary post-processing and analysis software [4] that used the so-called Equidistant Method [10] for simulation of hip motion and detection of extra-articular impingement in early hip motion. This method was specifically developed for virtual analysis of hip impingement and was previously used for patients with anterior femoroacetabular impingement (FAI) [4]. It allows stepwise analysis of bone-on-bone impingement, similar to other collision detection software [11, 12]. This software is based on a pelvic coordinate system and uses the so-called anterior pelvic plane as a frontal plane of reference [4]. During the simulation, the pelvis is in a fixed position, and the proximal femur is free to move. All three degrees of freedom are possible to test for the proximal femur. In a previous validation study, detection of an impingement conflict with a mean accuracy of less than 3° was reported (at an inter- and intra-observer agreement with an intraclass coefficient > 0.9 for external rotation and extension) [4].

Simulations of bone-on-bone impingement were performed for the following hip positions in stepwise increments of 10°:

- External rotation: 0 to 20°,
- Extension: 0 to 20°,
- Abduction/adduction: neutral position.

Maximum external rotation with neutral (0°) extension was measured at the point of impingement. Similarly, *maximum extension* with neutral external rotation (0°) was recorded at the point of impingement.

The simulated hip motions were chosen because these are important for the clinical posterior impingement test (also called apprehension test), which is performed supine applying hyperextension and passive external rotation [13]. The location of osseous impingement was tabulated as occurring in 3 extra-articular locations (Figs. 1, 2, and 3):

- Lesser trochanter,
- Greater trochanter, and
- Intertrochanteric area.

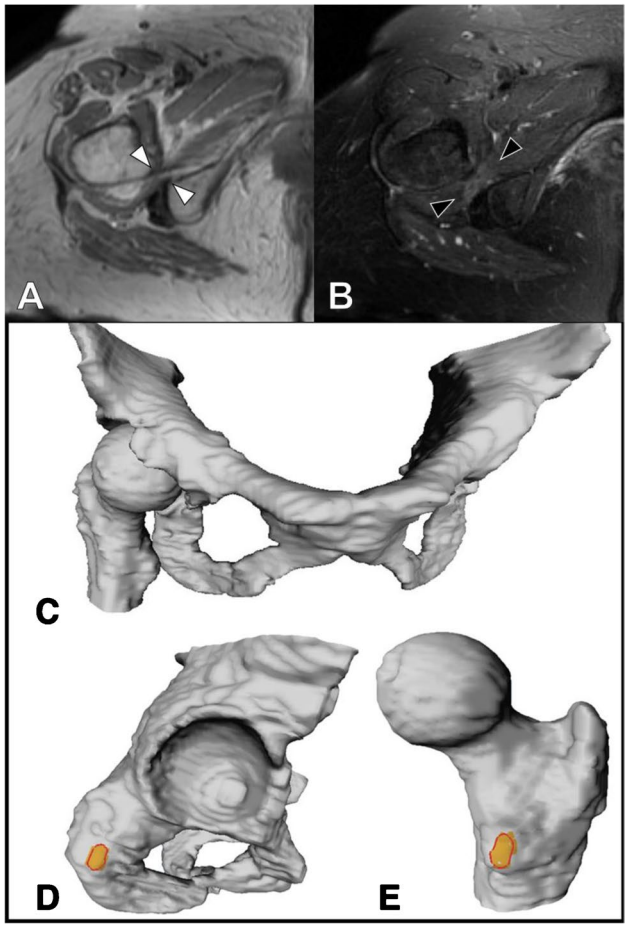

Fig. 1 **A** Axial PD-weighted and **B** T2-fat suppressed MRI of a symptomatic ischiofemoral impingement hip showing narrowed ischiofemoral and quadratus femoris spaces (white arrowheads) and thinning of the quadratus femoris muscle (black arrowheads). Corresponding 3D models of the same patient showing overlayed impingement location (colored area): **C** pelvis with articulated hip at isolated maximal extension, **D** ischium, **E** proximal femur

A report was created describing the following outcomes:

1. Frequency of impingement: how often impingement occurred at each hip position,
2. Location of impingement: simulated point of bone-on-bone contact,
3. Area of impingement: intersection between femoral and pelvic 3D models at a standardized 10° external rotation and 10° extension. This was done to compare the severity of bony collision at an early ROM in IFI vs. non-IFI hips.

Chi-squared test was performed to compare frequencies of impingement at different ROM between groups. Descriptive statistics were used to assess differences in impingement locations between groups. The frequency of LT involvement in early simulated bony contact was compared between groups using the Chi-squared test. The area of impingement was compared between IFI vs. non-IFI hips using Wilcoxon signed-rank test.

Results

A total of 16 hips (8 subjects) were examined for this study, comprising 7 IFI hips and 9 non-IFI hips. All subjects were female, with a mean age of 59.6±9.2 years. Significant differences were noted between the prevalence of soft tissue edema and symptoms between IFI vs. non-IFI hips ($P = 0.009$ for both). Cohort characteristics are outlined in Table 1.

Frequency of impingement

Simulation of hip external rotation and extension using MRI-based 3D models was possible for all 16 hips. No segmentations had to be changed by the second reviewing radiologist. As expected, impingement occurred more often in IFI hips for each of the simulated ROM combinations, being significant in the majority (5 out of 9 ROM combinations, $P < 0.05$). IFI hips showed 100% frequency of bony contact at 20° external rotation regardless of extension (Fig. 4). Notably, IFI hips also showed some frequency of bony contact at 0° external rotation with 10–20° extension. On the other hand, non-IFI hips showed low frequencies of bony contact at 10° external rotation regardless of extension, with a substantially increased frequency of bony contact at 20° external rotation (albeit lower than IFI hips).

Location of impingement

Impingement involved the LT significantly more often in IFI hips (overall $P < 0.001$, Fig. 5). Similar to differences in frequency of impingement, differences in LT involvement were seen at early degrees of external rotation and extension. At the earliest point of bony contact involving the LT, which was at 0° external rotation and 10° extension, it was involved in 29% of IFI hips, compared to 0% of non-IFI hips. At 20° external rotation and 20°extension, the absolute difference was even more pronounced with 86% vs. 44% involvement of the LT.

Initial bony contact location differed when simulating *maximum external rotation* and *maximum extension* of the hip. In *maximum external rotation*, the GT, intertrochanteric area, and both combined were involved in 14%, 57%, and 29% of IFI hips, respectively, vs. 67%, 33%, and 0% in non-IFI hips. Notably, the LT was not involved in any hips at *maximum external rotation*. In *maximum extension*, the LT, intertrochanteric area, and both combined were involved in 71%, 14%, and 14% of IFI hips, respectively, vs. 100%, 0%, and 0% in non-IFI hips. The GT was not involved in *maximum extension* in any hips.

Area of impingement

The simulated area of bone impingement was significantly different between IFI vs. non-IFI hips. At 10° extension/10° external rotation, impingement occurred in 86% of IFI hips

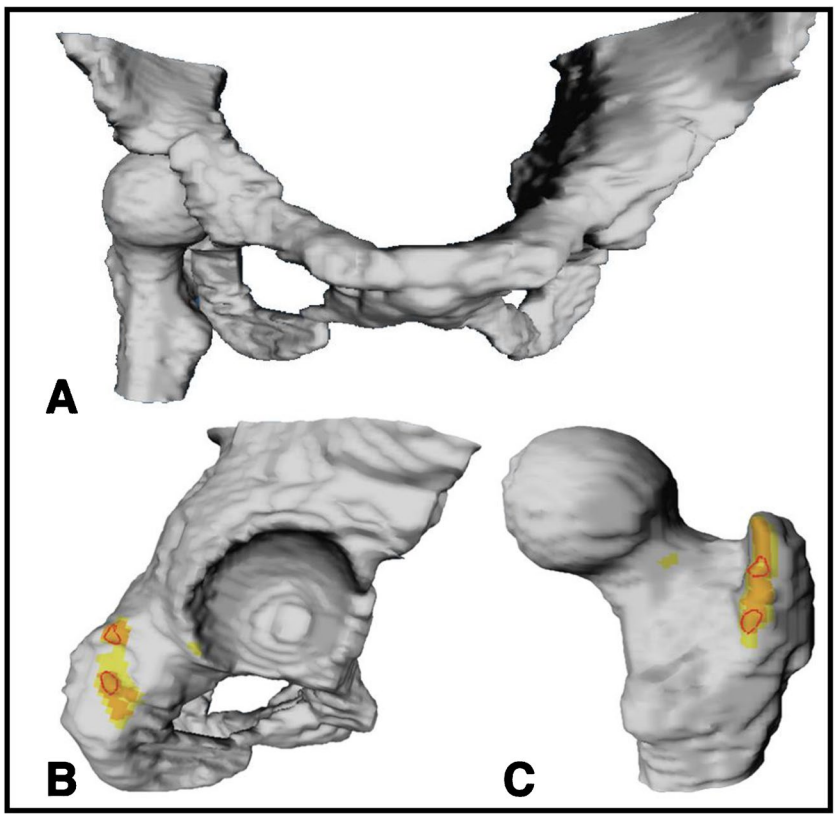

Fig. 2 Impingement of greater trochanter in a symptomatic ischiofemoral impingement hip. 3D models show impingement (colored area) in isolated hip maximal external rotation involving the ischium and greater trochanter: **A** pelvis with articulated hip, **B** ischium, **C** proximal femur

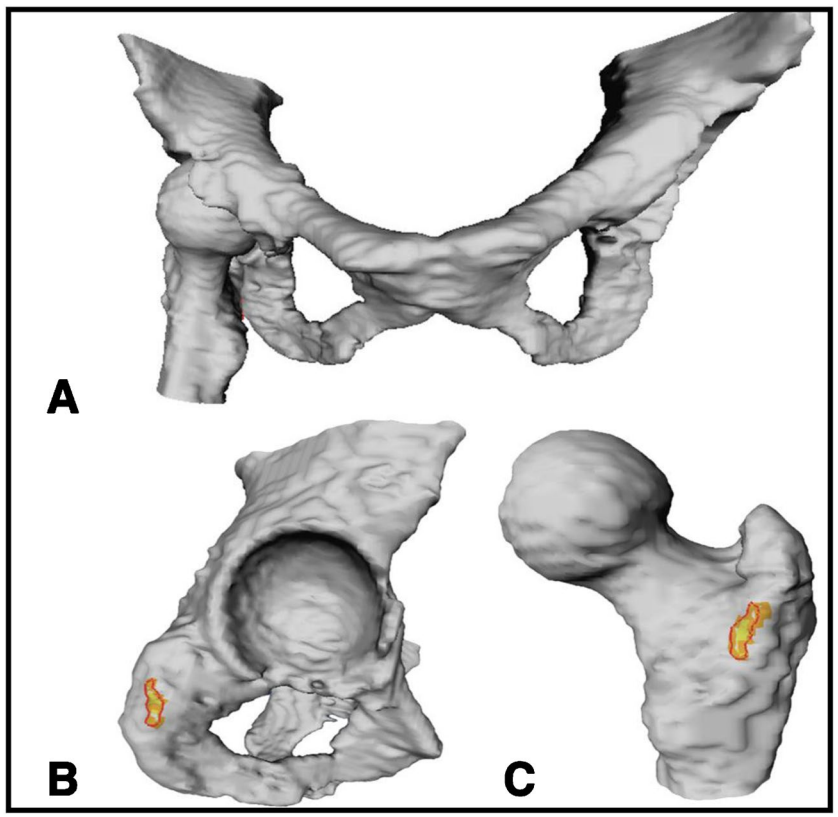

Fig. 3 Impingement of intertrochanteric area in a symptomatic ischiofemoral impingement hip. 3D models show impingement (colored area) in isolated hip maximal external rotation involving the ischium and intertrochanteric area: **A** pelvis with articulated hip, **B** ischium, **C** proximal femur

Table 1 Characteristics of study subjects

	IFI hips ($N = 7$)	non-IFI hips ($N = 9$)	P-value
Ischiofemoral space (mm)	12.7 ± 1.8	20.1 ± 2.5	< 0.0001
Quadratus femoris space (mm)	8.6 ± 1.6	13.9 ± 3.2	0.001
Presence of soft tissue edema (N, %)	4 (57%)	0 (0%)	0.009
Presence of symptoms (N, %)	4 (57%)	0 (0%)	0.009

IFI ischiofemoral impingement

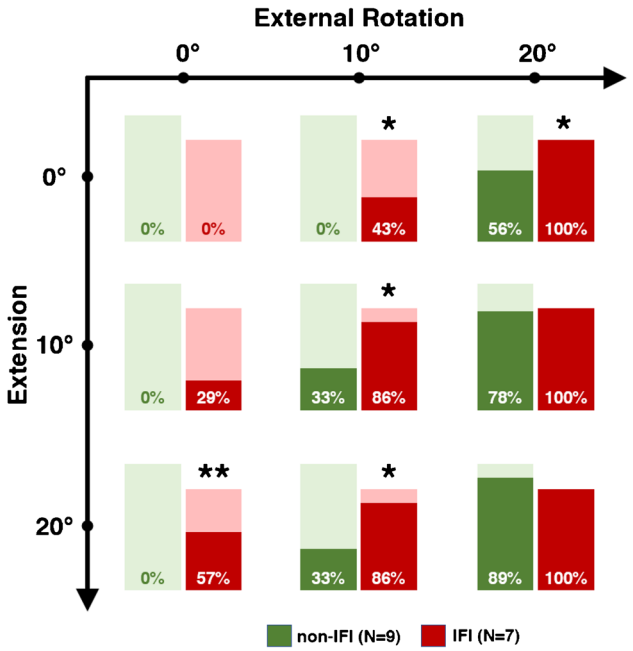

Fig. 4 Frequency of any bony contact at different degrees of external rotation and extension. Differences in relative frequency of impingement are seen between ischiofemoral impingement (IFI, red) and non-IFI hips (green) at all combinations of external rotation and extension. Percentages represent the frequency of impingement relative to the total cases in each group. *$P < 0.05$; **$P < 0.01$

compared to 33% of non-IFI hips ($P = 0.04$). At this simulated ROM, the area of bone impingement was significantly larger in IFI-hips vs. non-IFI hips ($P = 0.01$; 159 ± 121 mm^2 vs. 21 ± 45 mm^2, respectively) (Fig. 6).

Discussion

Our findings were (1) simulation of hip external rotation and extension showed a high frequency of ischiofemoral bony contact at 20° external rotation in IFI hips, regardless of extension; (2) simulated ischiofemoral bony contact frequently involved ischial tuberosity and LT, dependent on degree of hip extension, and GT and intertrochanteric area points of contact were noted; and (3) area of simulated impingement at early external rotation and extension was higher in IFI hips, conveying the severity of this phenomenon.

Prior studies have demonstrated the value of hip motion simulations using 3D models [4]. CT models of symptomatic patients with increased femoral version showed reduced conflict-free ROM at simulated extension and external rotation at 0° flexion [7]. That study also evaluated impingement location at 20° extension and 20° external rotation describing intra- and extra-articular impingement in patients with increased femoral version [7]. In another study,

Fig. 5 Schematic outlining locations of femoral impingement

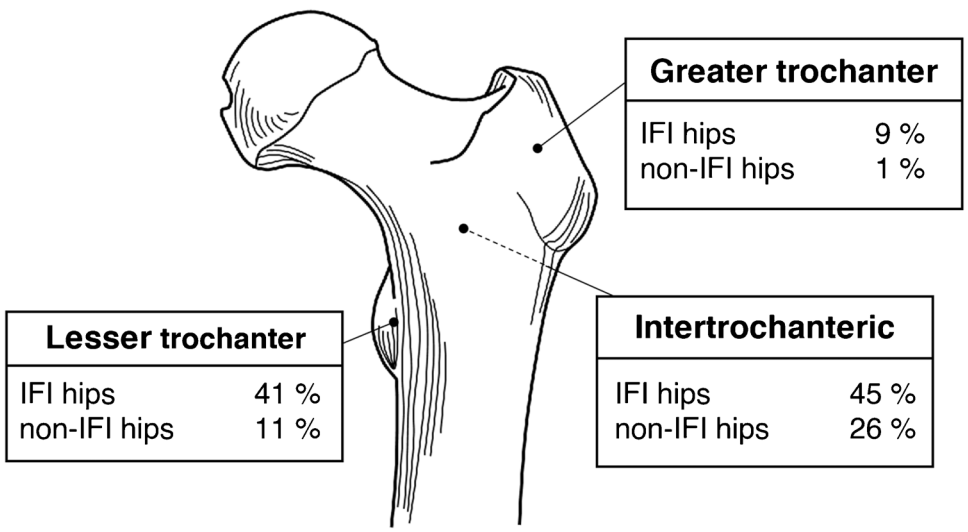

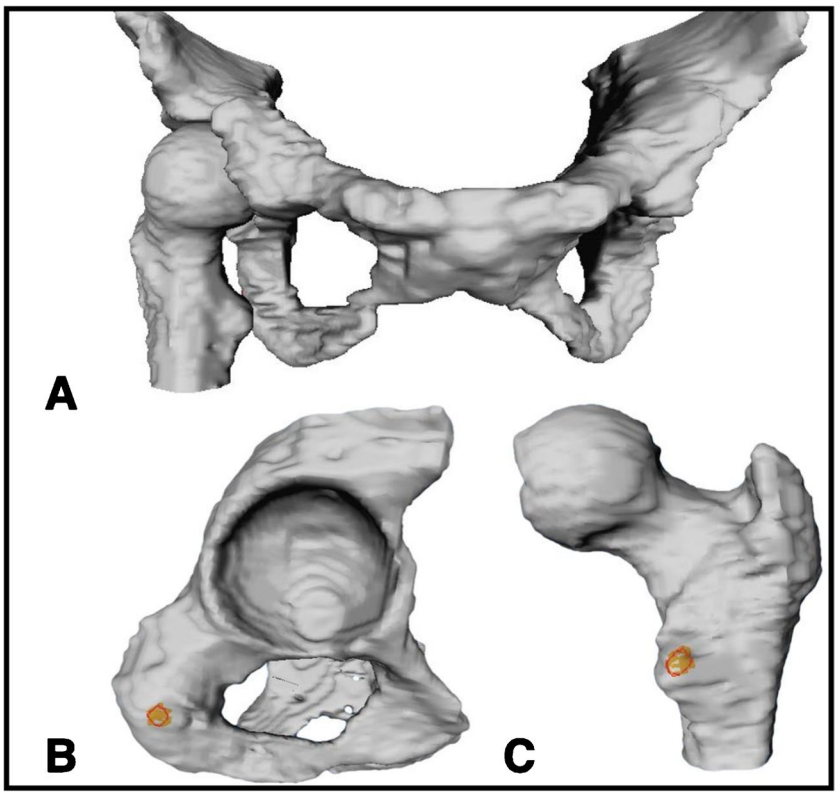

Fig. 6 Simulated impingement (colored area) in 10° external rotation/10° extension of a symptomatic ischiofemoral impingement hip, showing bony contact areas at ischial tuberosity and lesser trochanter: **A** pelvis with articulated hip, **B** ischium, **C** femur

a more posterior impingement zone on the acetabulum was noted in patients with post-Perthes deformities compared to normal controls or FAI patients [14]. To our knowledge, similar 3D MRI assessments of IFI have not been described.

We found a high frequency of simulated bony contact at 20° external rotation regardless of extension in IFI hips: 100% had impingement at 20° external rotation and 20° extension, which is comparable to the prior reported frequency of impingement (92%) [7]. This has partly been explored with ultrasound and MRI [6, 15], and reduced ischiofemoral and QF spaces with increased extension and adduction were examined, but the effect of isolated flexion-extension or thresholds for bony contact is unknown [16].

IFI hips also showed some frequency of bony contact at 0° external rotation with 10–20° of extension. Considering the usual degrees of forced extension during clinical tests, this finding is expected, as 10–20° may be considered as realistic maximum of forced extension [13]. In addition, we demonstrated that simulated impingement occurs beginning at 10° external rotation with minimal or no extension at all, which may be more sensitive than the posterior impingement test, which uses passive external rotation presumably beyond 10° [13]. Taken together, our findings confirm that bony contact can occur at early stages of external rotation and extension in IFI hips with as little as 10° of either.

We also found that in cases with bony contact, impingement involved the LT significantly more often in IFI hips. However, bony contact was also noted between ischial tuberosity vs. GT or intertrochanteric area. This is in keeping with evidence of reduced width between the GT vs. ischial tuberosity and hamstring origin in IFI hips [15]. Furthermore, the findings of our study are comparable to a prior study showing posterior impingement at LT or GT in symptomatic subjects with increased femoral version [7].

As a surrogate of bone contact severity, we measured the impingement area between pelvic and femoral 3D models. At 10° external rotation and 10° extension, this area was significantly higher in IFI hips. This finding could be relevant for optimizing therapy choices. Currently, different treatments for IFI patients have been described, ranging from physical therapy, ischiofemoral injections [17] to surgery [18–20]. Prior studies described LT resection with significantly reduced post-operative pain [21, 22]. Currently, no consensus on the best treatment for IFI is available [8]. 3D modeling could help analyze individual impingement location and help guide decision-making.

We found that impingement location differs between maximum external rotation and maximum extension. In isolated maximum external rotation, bony contact involves the GT and intertrochanteric area in IFI hips, without LT involvement. Conversely, at maximum extension, the LT is often involved. This indicates that some degree of extension is required for impingement to involve the LT, which was originally implicated in IFI [1]. Furthermore, our findings agree with observations of a potential role of GT in bony contact

[15]. Importantly, current evaluation for IFI relies on 2D MRI and measurements of ischiofemoral and QF spaces that are dependent on hip external rotation [6]. Therefore, objective diagnostic tools independent of hip position are desirable such as impingement simulation. Our findings may assist in surgical planning where LT resection is favored or indicate the need for more extensive osteotomies. This may be particularly relevant in cases where ROM analysis can prove the LT as the main contributor to IFI. Conversely, if the intertrochanteric area or GT is the dominant structure contacting the ischium, alternative surgical or conservative approaches may be considered.

Limitations of our study include a relatively small female cohort, lack of information on symptom duration and ROM, no knee images available to measure femoral version, and slightly lower image resolution of our images compared to previous CT-based studies. Furthermore, soft tissue impingement was not evaluated. Nonetheless, the dominant phenomenon in IFI arises from abnormal bony relationships, representing the main focus of our study and others evaluating hip ROM in pathologies other than IFI [4, 11].

In conclusion, 3D models derived from high-resolution MR images are feasible and enhance the analysis of posterior hip impingement in IFI. Extra-articular impingement occurs at higher frequency and earlier stages of external rotation and extension in IFI hips.

Declarations

Conflict of interest The authors declare no competing interests.

References

1. Torriani M, Souto SC, Thomas BJ, Ouellette H, Bredella MA. Ischiofemoral impingement syndrome: an entity with hip pain and abnormalities of the quadratus femoris muscle. AJR Am J Roentgenol. 2009;193(1):186–90.
2. Stafford GH, Villar RN. Ischiofemoral impingement. J Bone Joint Surg (Br). 2011;93(10):1300–2.
3. Bredella MA, Azevedo DC, Oliveira AL, Simeone FJ, Chang CY, Stubbs AJ, et al. Pelvic morphology in ischiofemoral impingement. Skelet Radiol. 2015;44(2):249–53.
4. Tannast M, Kubiak-Langer M, Langlotz F, Puls M, Murphy SB, Siebenrock KA. Noninvasive three-dimensional assessment of femoroacetabular impingement. J Orthop Res. 2007;25(1):122–31.
5. Schröder RG, Reddy M, Hatem MA, Gómez-Hoyos J, Toye L, Khoury A, et al. A MRI study of the lesser trochanteric version and its relationship to proximal femoral osseous anatomy. J Hip Preserv Surg. 2015;2(4):410–6.
6. Vicentini JRT, Martinez-Salazar EL, Simeone FJ, Bredella MA, Palmer WE, Torriani M. Kinematic MRI of ischiofemoral impingement. Skeletal Radiol. 2021;50(1):97–106.
7. Lerch TD, Zwingelstein S, Schmaranzer F, Boschung A, Hanke MS, Todorski IAS, et al. Posterior extra-articular ischiofemoral impingement can be caused by the lesser and greater trochanter in patients with increased femoral version: dynamic 3D CT-based hip impingement simulation of a modified FABER test. Orthop J Sports Med. 2021;9(5):2325967121990629.
8. Singer AD, Subhawong TK, Jose J, Tresley J, Clifford PD. Ischiofemoral impingement syndrome: a meta-analysis. Skelet Radiol. 2015;44(6):831–7.
9. Yushkevich PA, Piven J, Hazlett HC, Smith RG, Ho S, Gee JC, et al. User-guided 3D active contour segmentation of anatomical structures: significantly improved efficiency and reliability. Neuroimage. 2006;31(3):1116–28.
10. Puls M, Ecker TM, Tannast M, Steppacher SD, Siebenrock KA, Kowal JH. The Equidistant Method - a novel hip joint simulation algorithm for detection of femoroacetabular impingement. Comput Aided Surg. 2010;15(4-6):75–82.
11. Bedi A, Dolan M, Hetsroni I, Magennis E, Lipman J, Buly R, et al. Surgical treatment of femoroacetabular impingement improves hip kinematics: a computer-assisted model. Am J Sports Med. 2011;39(Suppl):43S–9S.
12. Bouma H, Hogervorst T, Audenaert E, van Kampen P. Combining femoral and acetabular parameters in femoroacetabular impingement: the omega surface. Med Biol Eng Comput. 2015;53(11):1239–46.
13. Tannast M, Siebenrock KA, Anderson SE. Femoroacetabular impingement: radiographic diagnosis--what the radiologist should know. AJR Am J Roentgenol. 2007;188(6):1540–52.
14. Tannast M, Hanke M, Ecker TM, Murphy SB, Albers CE, Puls M. LCPD: reduced range of motion resulting from extra- and intraarticular impingement. Clin Orthop Relat Res. 2012;470(9):2431–40.
15. Singer A, Clifford P, Tresley J, Jose J, Subhawong T. Ischiofemoral impingement and the utility of full-range-of-motion magnetic resonance imaging in its detection. Am J Orthop (Belle Mead NJ). 2014;43(12):548–51.
16. Finnoff JT, Bond JR, Collins MS, Sellon JL, Hollman JH, Wempe MK, et al. Variability of the ischiofemoral space relative to femur position: an ultrasound study. PM R. 2015;7(9):930–7.
17. Backer MW, Lee KS, Blankenbaker DG, Kijowski R, Keene JS. Correlation of ultrasound-guided corticosteroid injection of the quadratus femoris with MRI findings of ischiofemoral impingement. AJR Am J Roentgenol. 2014;203(3):589–93.
18. Gollwitzer H, Banke IJ, Schauwecker J, Gerdesmeyer L, Suren C. How to address ischiofemoral impingement? Treatment algorithm and review of the literature. J Hip Preserv Surg. 2017;4(4):289–98.
19. Hernando MF, Cerezal L, Pérez-Carro L, Canga A, González RP. Evaluation and management of ischiofemoral impingement: a pathophysiologic, radiologic, and therapeutic approach to a complex diagnosis. Skelet Radiol. 2016;45(6):771–87.
20. Nakano N, Shoman H, Khanduja V. Treatment strategies for ischiofemoral impingement: a systematic review. Knee Surg Sports Traumatol Arthrosc. 2020;28(9):2772–87.
21. Hatem MA, Palmer IJ, Martin HD. Diagnosis and 2-year outcomes of endoscopic treatment for ischiofemoral impingement. Arthroscopy. 2015;31(2):239–46.
22. Hernandez A, Haddad S, Nuñez JH, Gargallo-Margarit A, Sallent A, Barro V. Ischiofemoral impingement syndrome: outcomes of endoscopic resection of the lesser trochanter. Clin Orthop Surg. 2017;9(4):529–33.